

Study of the Local Structure in Vitreous Chalcogenides via Measurement of Asymmetry of the Electric-Field-Gradient Tensor

J. Szeftel and H. Alloul

Laboratoire de Physique des Solides, Université Paris-Sud, 91405 Orsay, France

(Received 29 January 1979)

The electric-field-gradient asymmetry parameter has been measured in several vitreous chalcogenides at arsenic sites which undergo a strong quadrupolar coupling. Results in vitreous As_2S_3 and As_2Se_3 reveal a cylindrical local symmetry which contrasts with the distortion associated with the lamellar structure crystalline As_2S_3 . However, in amorphous $\text{As}_{75}\text{Te}_{75}$ and $\text{As}_{45}\text{Te}_{55}$ the local environment of arsenic displays a sizable distortion.

In contrast to the case of crystalline materials, diffraction techniques cannot provide, in glasses, a complete description of the local order. X rays have been extensively applied to vitreous As-S,¹ As-Se,² and As-Te (Ref. 3) compounds. In vitreous As_2S_3 and As_2Se_3 , the question as to whether the amorphous lattice consists of planes of As- X_3 pyramids ($X=\text{S}$ or Se) as in crystalline As_2S_3 (orpiment) or a random covalent network of As- X_3 units linked by an X atom remains controversial. The new information on the local environment of arsenic, to be presented here, has been derived from an investigation of the symmetry properties of the electric field gradient (EFG) arising from bonding electrons of the As atom. The EFG traceless tensor interacts with the quadrupole moment Q of ^{75}As , which has a spin I of $\frac{3}{2}$, through the quadrupole coupling H_Q and is defined in terms of its largest eigenvalue q_{zz} ($q_{zz} \geq q_{xx} \geq q_{yy}$ referred to the three eigenvalues of the EFG tensor) and a dimensionless coefficient $\eta = (q_{xx} - q_{yy})/q_{zz}$, ranging from 0 to 1. Rubinstein and Taylor⁴ have measured q_{zz} in amorphous As_2S_3 and As_2Se_3 . Their results confirm the x-ray scattering analysis that the pyramidal structure is retained in those glasses. However, the asymmetry parameter η , which is of major importance concerning the local environment of arsenic because it reflects the symmetry of the spatial distribution of electrons surrounding the As atom and vanishes in case of local cylindrical symmetry, remains unknown. The measurement of η , presented here, provides an insight into the local structure of vitreous chalcogenides which is not available from other techniques and it enables us to propose a description of the arrangement of As- X_3 pyramids.

Although the existence of the particular resonance detected here has been reported once in crystalline metallic compounds,⁵ the theoretical treatment included therein does not afford a line-

shape analysis. This Letter contains, then, the first application of the method in order to extract structural information. For this purpose, a complete calculation of the spectrum for $I = \frac{3}{2}$ is summarized in the following.

In As chalcogenides, H_Q is so strong (several tens of MHz) that no conventional NMR measurement can be performed. q_{zz} and η might still be obtained from Zeeman perturbation of pure quadrupole resonance as sketched on Fig. 1. In zero magnetic field ($H = 0$), a single resonance, referred to as pure quadrupole, occurs at a frequency ω_Q given by⁶

$$\omega_Q = Q\rho q_{zz}/2\hbar, \quad \rho = (1 + \eta^2/3)^{1/2}. \quad (1)$$

Since ω_Q alone cannot yield both q_{zz} and η , a small Zeeman perturbation ($H \neq 0$ on Fig. 1) is applied which lifts the degeneracy. Four resonances at frequencies ω_i ($i = 1, 2, 3, 4$) close to ω_Q are then observed and could afford a complete determination of q_{zz} and η .⁶ This latter method is valid for a single crystal and obviously breaks down in a glass where a major problem arises from the random fluctuations of ω_Q from site to site induced by the structural disorder as pointed out in Ref. 4. The four narrow resonances observed at ω_i in a single crystal turn into a broad unresolved spectrum centered at the mean ω_Q

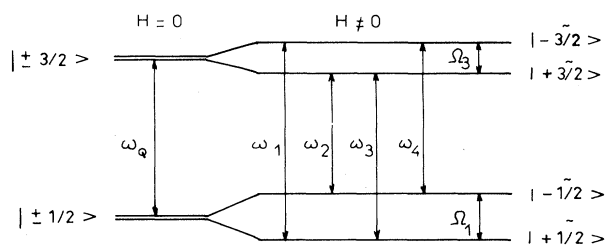


FIG. 1. Energy-level diagram for a nuclear spin $I = \frac{3}{2}$ in presence of a strong quadrupole coupling and, respectively, zero and nonzero Zeeman perturbation.

value. The successful η measurement reported here relies upon observation of resonance at frequencies Ω_1 and Ω_3 (see Fig. 1) small with respect to ω_Q . Expressions⁶ for Ω_1 and Ω_3 , valid to first order in H , are

$$\Omega_i = \gamma H [a_i^2 \cos^2 \theta + (b_i^2 + c_i^2 + 2b_i c_i \cos 2\Phi) \sin^2 \theta]^{1/2}. \quad (2)$$

Subscript i refers, respectively, to 1 and 3, γ is the gyromagnetic ratio of the considered nucleus, θ and Φ are the polar angles of the field with respect to the principal axis of the EFG tensor. The key point is that, as coefficients a_i , b_i , and c_i given in (Ref. 6) are functions of η only, the determination of η turns out to be decoupled from that of q_{zz} . As in a polycrystalline sample, the local principal axis in a glass may take any direction with respect to \bar{H} . The resulting powder spectrum has been calculated for each η value, taking account of the θ and Φ dependence of both the $|\bar{m}\rangle$ states and the transition probabilities. The calculated intensity of line 3 has been found to be so weak relative to that of line 1 (it actually vanishes if $\eta=0$) that we have failed to detect any resonance associated with line 3. Therefore i will be dropped henceforth and only line 1 will be considered. At a frequency Ω , the spectrum $S_\eta(r)$, where $r = \gamma H / \Omega$, is bounded by two limits r_m and r_M ($r_m \leq r \leq r_M$) and has a logarithmic divergence at r_p . Expressions for these parameters are as follows (complete calculations will be given elsewhere):

$$\begin{aligned} r_m &= [1 + (1 + \eta)/\rho]^{-1}, & r_p &= [1 + (1 - \eta)/\rho]^{-1}, \\ r_M &= (2/\rho - 1)^{-1}. \end{aligned} \quad (3)$$

Two spectra corresponding to $\eta=0.1$ and $\eta=0.5$ are plotted in Fig. 2 to illustrate qualitatively their η dependence. As η increases, the area

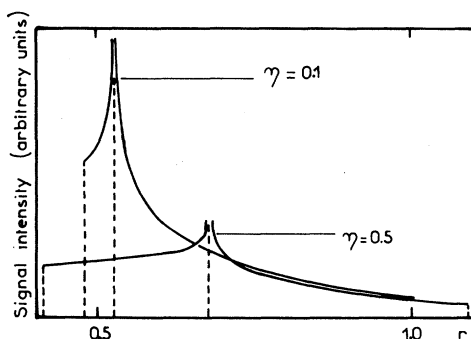


FIG. 2. Spectra (solid lines) calculated for two values of η , corresponding to the same number of nuclei.

under the curve near r_p and hence the sensitivity at r_p strongly diminish, whereas the values of r_M and r_m , respectively, increase and decrease. Consequently, in case of a distribution of η values, the contribution at $r < 0.5$ and $r > 1$ will come from higher η values while the position of the peak will be influenced mainly by the lower values of the distribution.

Measurements have been carried out at 4.2 K on samples quenched from the melt by monitoring, at fixed Ω , the spin echo of ^{75}As as a function of H with a phase-coherent pulse spectrometer. The considerable width of the spectra (of the same order as Ω), evident in Fig. 2, is responsible for the difficulty of the experiment. Therefore, long integration is required which has fortunately been made much easier by the relatively short spin-lattice relaxation time. (This rapid relaxation is a general property of the glassy state.⁷ ^{75}As spectra obtained in vitreous As_2S_3 , As_2Se_3 , $\text{As}_{45}\text{Te}_{55}$, and $\text{As}_{25}\text{Te}_{75}$ have been plotted in Fig. 3. In all cases, the experiment, carried out at two different frequencies, has yielded an Ω -independent pattern, which supports the validity of the first-order treatment summarized above. In addition, in $\text{As}_x\text{Te}_{100-x}$ compounds where ω_Q is unknown, it can be inferred to be much larger than the higher Ω value used (10.3 MHz). It is not possible to obtain a good fit with the data in all cases by using a single η value. The required distribution $f(\eta)$ has been determined by a trial-and-error method so that $\int_0^1 f(\eta) S_\eta(r) d\eta$ provides the best fit with experiment. The peak of the resonance signal enables us to infer from the r_p expression [see Eq. (3)] the peak value η_{1m} of $f(\eta)$. A Gaussian distribution $\exp[-(\eta - \eta_{1m})^2 / 2\sigma_1^2]$ is then conveniently chosen as a first trial function for $f(\eta)$. For $\text{As}_x\text{Te}_{100-x}$, a good fit [solid lines in Figs. 3(c) and 3(d)] is obtained with $\eta_{1m} = 0.34 \pm 0.03$ and $\sigma_1 = 0.14$ in $\text{As}_{45}\text{Te}_{55}$ and with $\eta_{1m} = 0.3 \pm 0.03$ and $\sigma_1 = 0.14$ in $\text{As}_{25}\text{Te}_{75}$. (However, a Lorentzian curve centered at η_{1m} with of a width of order σ_1 gives as good a fit.) The best choice of η_{1m} and σ_1 corresponds to $\eta_{1m} = 0.12 \pm 0.02$ and $\sigma_1 = 0.04$ in As_2S_3 and to $\eta_{1m} = 0.14 \pm 0.02$ and $\sigma_1 = 0.07$ in As_2Se_3 , respectively, and yields the dashed curves on Figs. 3(a) and 3(b). Modification of η_{1m} and an increase in σ_1 shift and broaden the calculated curve beyond the experimental spectrum without improving the fit for $r > 0.75$ and $r < 0.5$, which demonstrates the presence of As sites with large η values. To account for those sites, a second Gaussian distribution $\exp[-(\eta - \eta_{2m})^2 / 2\sigma_2^2]$ of lower weight is

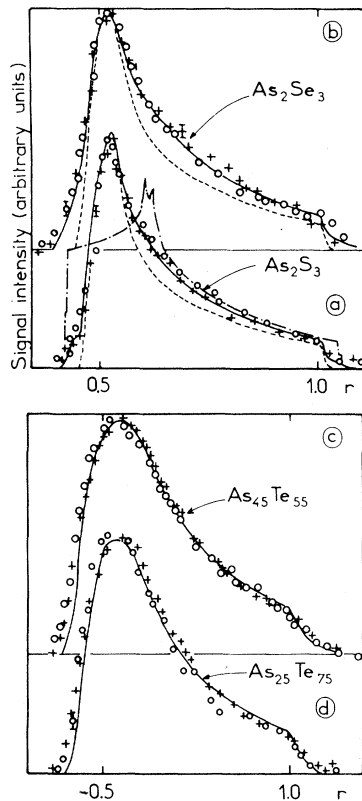


FIG. 3. ^{75}As spectra recorded in four vitreous chalcogenides at 5.9 MHz (circles) and 10.3 MHz (crosses). The powder spectrum calculated with η values of orpiment is plotted as dashed-dotted lines. Solid lines indicate the best fit. When two Gaussian distributions are needed to obtain the best fit, the contribution of the distribution of higher weight is plotted as dashed lines.

added to the former one, which gives the solid lines in Figs. 3(a) and 3(b). The values of the relevant parameters are $\eta_{2m} = 0.36$ and $\sigma_2 = 0.07$ in As_2S_3 , and $\eta_{2m} = 0.45$ and $\sigma_2 = 0.14$ in As_2Se_3 , and the relative weights associated with the first Gaussian distribution (η_{1m}, σ_1) are, respectively, equal to 70% in As_2S_3 and 60% in As_2Se_3 . In view of the limited accuracy, the determination of η_{2m} and σ_2 is far from being reliable since using a rectangular distribution ranging from $\eta \sim 0.2$ to $\eta \sim 0.6$ yields nearly as good a fit.

In orpiment, two values of η ($\eta = 0.34, 0.37$) are found⁴ which correspond to distorted As-S_3 pyramids. The spectrum calculated with these values is plotted on Fig. 3(a) as dashed-dotted lines to emphasize the marked difference with the glass. In orpiment, the pyramids share alternatively an edge or a corner of the triangle formed by three S's. Hence, the different roles played on

one hand by the linking sulfur and on the other hand by the common edge result in unequal apex angles between different As-S bonds. From our data, it can be inferred that the distorted pyramids of orpiment are present but comprise a minority of the As atoms in amorphous As_2S_3 , since most As atoms (70%) are located at the apex of an almost regular pyramid ($\eta_m = 0.12$ is close to zero). By lifting the constraint of the particular branching of pyramids in orpiment responsible for the distortion and postulating a covalent random network of pyramids linked to one another by one S corner only, one accounts for both the high local symmetry of most As sites in the glass and for the lower density of the glass relative to that of the crystal. Indeed, this structure is more open than that of the crystal, which decreases interaction between pyramids and restores regular As-S_3 units.⁵ It then appears that only 30% of As sites showing substantial distortion are reminiscent of the lamellar structure of orpiment. Similar conclusions as for vitreous As_2S_3 can be derived for the structure of As_2Se_3 by merely substituting As-Se_3 pyramids for As-S_3 ones. The higher σ values observed in As_2Se_3 relative to As_2S_3 reveal that the fluctuations in bond angles of the arsenic atom induced by the structural disorder are more important in As_2Se_3 . This could be due to strains, inasmuch as our As_2Se_3 sample was rapidly quenched from the melt.

On the basis of their x-ray scattering data, Cornet and Rossier³ have arrived at the following conclusions: (i) There is no As site of octahedral symmetry in amorphous $\text{As}_x\text{Te}_{100-x}$ compounds unlike crystalline As_2Te_3 ; this conclusion is supported by our work since no strong and narrow NMR signal occurs at $r = 1$.⁹ (ii) For $x < 40$, arsenic atoms occupy the apex of a As-Te_3 pyramid (those sites are likely to give rise to the signal reported here). (iii) For $x > 40$, the extra proportion of As atoms ($x - 40$) is claimed to form As-As pairs referred to as "locks." Because of the lack of sensitivity we have failed to detect any contribution from these locks in $\text{As}_{45}\text{Te}_{55}$, where they represent, in principle, 11% of the total amount of arsenic. A further experiment on a sample with high As content ($\text{As}_{60}\text{Te}_{40}$, for instance) is hence required to study the local structure of As atoms belonging to these locks. The most surprising result is the absence in vitreous $\text{As}_x\text{Te}_{100-x}$ compounds of As sites of high symmetry in distinction of glassy As_2S_3 and As_2Se_3 , which is ascribed to the particular chemical

properties of Te. As emphasized in Ref. 3, the angles between the different bonds of As and Te are smaller than corresponding angles of As and, respectively, S in As_2S_3 and Se in As_2Se_3 . This property tends to produce, in vitreous $\text{As}_x\text{Te}_{100-x}$ compounds, a more compact structure which favors strong chemical interaction between As-Te₃ pyramids and hence angular distortion.

The results obtained here lead to a description of the major part of the structure in vitreous As_2S_3 and As_2Se_3 as constituting an open, locally symmetric, random covalent network, while the structure of glassy $\text{As}_x\text{Te}_{100-x}$ compounds is more close packed and thus distorted. Hence it would be interesting to reinterpret the x-ray diffraction diagrams by using the conclusions reported here. Further calculations of the EFG tensor based on atomic orbital functions might combine the σ data of this paper and the ω_Q variations given in Ref. 4 to derive fluctuations of arsenic bond angles. Finally, the method developed here can be applied to other nuclei embedded in nonoriented media and having large Q .

The authors thank P. Monod, who suggested the

experiment, and J. Cornet, who supplied all the samples used here and gave useful explanations on his own work. Laboratoire de Physique des Solides is a Laboratoire associé au Centre National de Recherches Scientifiques.

¹S. Tsuchihashi and Y. Kawamoto, *J. Non-Cryst. Solids* **5**, 286 (1971).

²A. L. Renninger and B. L. Averbach, *Phys. Rev. B* **8**, 1507 (1973).

³J. Cornet and D. Rossier, *J. Non-Cryst. Solids* **12**, 85 (1973).

⁴M. Rubinstein and P. C. Taylor, *Phys. Rev. B* **9**, 4258 (1974).

⁵S. Wada and K. Asayama, *J. Phys. Soc. Jpn.* **34**, 1163 (1973).

⁶T. P. Das and E. L. Hahn, in *Solid State Physics*, edited by F. Seitz and D. Turnbull (Academic, New York, 1958), Suppl. 1.

⁷J. Szeftel and H. Alloul, *J. Non-Cryst. Solids* **29**, 253 (1978).

⁸On the basis of chemical arguments, an isolated regular pyramid is more stable than a distorted one.

⁹At a site of octahedral symmetry, H_Q vanishes and the nuclear resonance occurs as usual at $\Omega = \gamma H$.

Lattice-Parameter Changes due to Au Dissolution in Pb

W. K. Warburton^(a) and S. C. Moss

Physics Department, University of Houston, Houston, Texas 77004

(Received 11 September 1978)

A careful measurement of the lattice parameters of pure Pb and a Pb+(0.0918 at.% Au) sample after a quench and equilibrium annealing cycle shows that Au in both monomer and "tetramer" defect states produces lattice contraction with the "tetramer" somewhat remarkably having the larger effect per atom. The observed monomer contraction suggests that the majority site occupancy for Au is substitutional and that the rapid Au diffusion must therefore involve a substitutional-interstitial mechanism.

The Pb(Au) system has been long known for its ultrafast diffusion behavior^{1,2} which has been generally considered to result from an interstitial migration mechanism.^{3,4} More recent work demonstrates that further complexity exists, with the Au forming at least three equilibrium defects having one, two, and probably four Au atoms, respectively^{5,6} (Au_1 , Au_2 , and Au_4). Actually, the existence of the Au_n , $n > 2$, defect, while not in doubt, has not been absolutely determined at $n = 4$. We here merely accept the judgment of Ref. 6 that Au_4 is the most likely candidate. Since this situation is unique among diffusion systems studied to date and since it has been demonstrated that an appropriate quench can capture the system essentially completely in the Au_4 state,^{6,7} the possibility appeared to exist that Huang diffuse

x-ray scattering⁸ might be used to obtain symmetry information about these defects. As a preliminary to such a measurement we have made a careful measurement of the change of lattice parameter, $\Delta a/a$, since this is both a measure of the strain introduced by the defects and a requirement for an estimate of the Huang scattering.

Single crystals of pure Pb and Pb+(9.18×10⁻² at.% Au) were grown by the Bridgman technique in boats of reactor-grade graphite using 99.9999%-purity Cominco Pb and 99.99%-purity Research Organic/Inorganic Chemical Corporation Au. Wafer specimens were formed by sparkcutting, following a Laue orientation to within about ½° of the [110] axis. Since Pb is particularly susceptible to surface damage, the wafers were chemically planed to obtain a flat face within about 0.05°